Aerial imaging study of the mask-induced line-width roughness of EUV lithography masks

Antoine Wojdyla[1,*], Alexander Donoghue[1], Markus P. Benk[1], Patrick P. Naulleau[1] and Kenneth A. Goldberg[1]
[1]Lawrence Berkeley National Laboratory, 1 Cyclotron Road, Berkeley, CA 94720 (USA)

ABSTRACT

EUV lithography uses reflective photomasks to print features on a wafer through the formation of an aerial image. The aerial image is influenced by the mask's substrate and pattern roughness and by photon shot noise, which collectively affect the line-width on wafer prints, with an impact on local critical dimension uniformity (LCDU). We have used SHARP, an actinic mask-imaging microscope, to study line-width roughness (LWR) in aerial images at sub-nanometer resolution. We studied the impact of photon density and the illumination partial coherence on recorded images, and found that at low coherence settings, the line-width roughness is dominated by photon noise, while at high coherence setting, the effect of speckle becomes more prominent, dominating photon noise for exposure levels of 4 photons/nm^2 at threshold on the mask size.

Keywords: EUV lithography, LER, LWR, actinic inspection, LCDU, X-Ray Microscopy, photon noise, partial coherence, power-spectral density, speckle, metrology, real-space imaging

1. INTRODUCTION

As extreme ultraviolet (EUV) lithography pushes lithographic resolution closer to the atomic scale, the specifications on critical dimension uniformity (CDU) are becoming more stringent. That is especially true for local CD uniformity (LCDU), which is a direct manifestation of the resist line-edge roughness (LER).

Though often considered within the context of the well-known resolution, LER and sensitivity (RLS) trade-off for photoresists, the final LER in printed features (Figure 1, right) arises from chemical processes in the resist, and from imperfections of the mask, transferred to the aerial image. These include pattern roughness (Figure 1, left) and the influence of speckle (i.e. phase roughness). Phase effects come from mask and multilayer roughness, and can only be seen in the actinic imaging. (Figure 1, center).

Extreme Ultraviolet (EUV) Lithography VII, edited by Eric M. Panning, Proc. of SPIE Vol. 9776, 97760H · © 2015 SPIE · CCC code: 0277-786X/15/$18 · doi: 10.1117/12.2219513

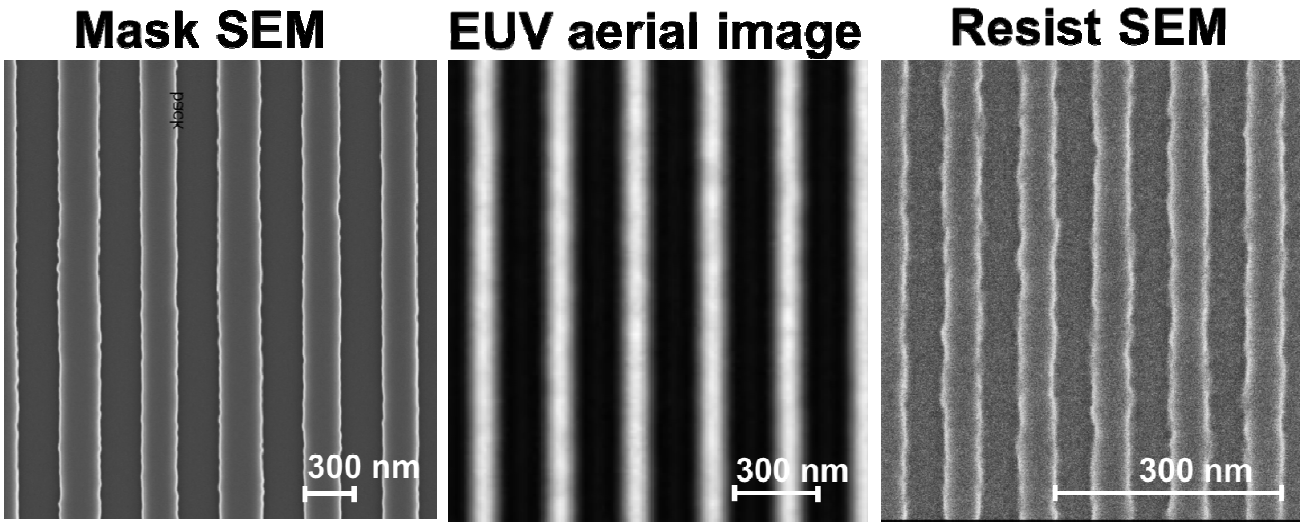

Figure 1. Pattern transfer in EUV lithography, from mask to wafer. Imperfections of the pattern on the photo-mask and intrinsic mask blank roughness are among the parameters that affect the final line-edge roughness on a printed wafer (these samples have similar yet different critical dimensions; they're for illustration purpose only.)

Because of the reflective nature of EUV photomasks, aerial images are highly sensitive to substrate roughness, which is typically on the order of 2-Å-RMS [1]. Depending on the deposition technique, substrate roughness is replicated into the reflective multilayer coating, causing phase errors that appear as speckle under coherent illumination conditions (figure 2.) In most cases, decreasing the illumination coherence decreases the speckle contrast.

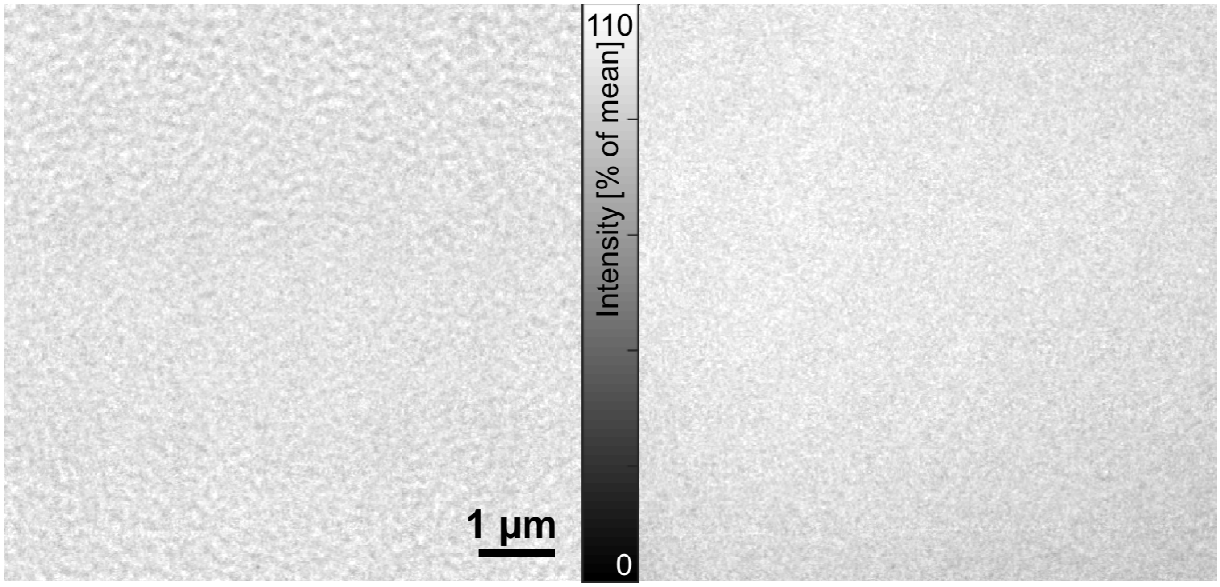

Figure 2. Aerial images of a typical EUV photo-mask blank, under coherent (left) and incoherent illumination (right.) With coherent illumination, the speckle caused by mask roughness can clearly be distinguished. Both images have a vertical focal gradient caused by the off-axis imaging conditions.

Early studies of aerial image LER by Naulleau and colleagues have focused on setting relevant tolerances through simulations [2], predicting the effects of replicated surface roughness on aerial images [3], and finding correlations between LER on independent wafer prints [4]. Later authors made indirect measurements of the mask-induced LER by printing [5,6]: they found that speckle could be replicated, but only for mask-roughness well above current

manufacturing capabilities. More recently, the aerial image LER roughness has been studied with an actinic microscope (SHARP) on a mask blank with a roughness gradient [7].

Mask substrate roughness is hard to improve and difficult to quantify in practice. Since phase roughness causes complex interactions, it is important to develop a metrology to perform the experimental evaluations of the aerial image LWR. Actinic aerial image measurements can help us to study the driving factors behind the formation of aerial image line-edge roughness, isolating the contributions of substrate roughness and photon shot noise, and providing feedback for mask manufacturers to improve over time.

2. DATA COLLECTION

We used the SHARP EUV mask-imaging microscope at Lawrence Berkeley National Laboratory [8] to record aerial images of a patterned EUV photomask. SHARP emulates the imaging properties of current and future generations of EUV lithography scanners. It is a synchrotron-based microscope that records real-space images with monochromatic, 13.5-nm-wavelength light ($E/\Delta E = 1450$) using diffractive Fresnel zone plate lenses. Its Fourier synthesis illuminator allows full coherence control, providing conventional and engineered illuminations.
In recent defect-imaging studies, SHARP has been shown to faithfully predict wafer printing at current EUV generations. [9]. SHARP's real-space imaging enables it to perform aerial image measurements of line-width, and LER or LWR.

The photomask used for this study is a standard EUV reflective Mo/Si multilayer blank patterned with absorber to form line-and-space test patterns, including a field of 200-nm-CD lines with 1:1 line-to-space ratio (in this paper, all dimensions are expressed in mask units.)

Images of the patterned field were acquired using a 0.33-4xNA lens at best focus. Figure 3 shows image details from the study. We varied (1) the exposure time from 5 seconds to 40 seconds to probe the influence of photon shot noise in the measurement, and (2) the partial coherence of the illumination, σ, from 0.3 to 0.8 to vary the image slope. (The partial coherence factor is defined as $\sigma = NA_{illum}/NA_{lens}$, with $\sigma = 0$ being the fully coherent illumination condition.)

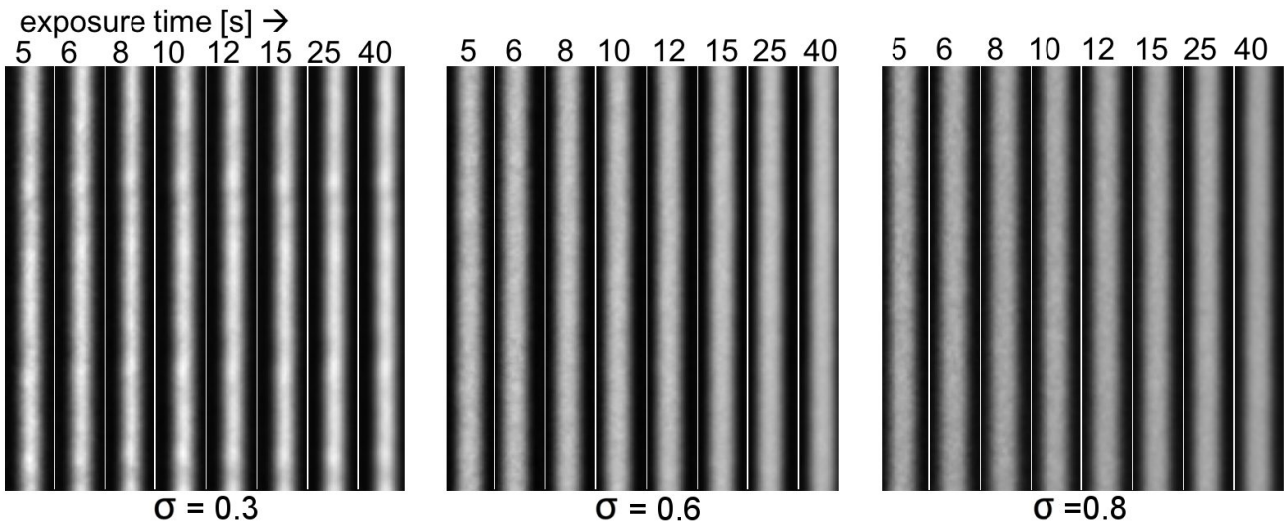

Figure 3. Sample 160 nm (4xCD) bright line from the collected aerial images, with various exposure times and partial coherence. Photon noise decreases with exposure time, while a decrease in coherence blurs out speckle (intensity levels are linearly adjusted with the exposure time for comparison.)

The images were cropped to a $5x5\mu m^2$ area, where the imaging performance is diffraction limited, while the vertical focal gradient (arising from the off-axis configuration) and sample illumination uniformity cause CD variations less than 1% along the length of the line, covering about 14 contiguous lines (independent and identically distributed (*i.i.d.*)) For each exposure time and illumination condition, measurements were repeated ten times to build a statistical ensemble.

3. LINE-EDGE RETRIEVAL PROCEDURE

Aerial image measurements are intrinsically continuous, and edge extraction occurs by interpolating the gray levels. This is different from the way in which edges are extracted from mask or wafer-print SEM micrographs. In SHARP, the effective pixel width corresponds to 15-nm in mask units, well below the resolution of the imaging element. To perform a consistent analysis of the data throughout this study, we set an intensity threshold level to yield an average line-width with a nominal 160-nm line-width in the bright region. This width was chosen to allow for a comparison between the various partial coherence settings. The threshold level is adjusted for each dataset to maintain the nominal width as the line shape and intensity varies. To assess nm-scale edge-position information, it is necessary to perform a row-by-row linear interpolation of the images, and determine the threshold-crossing positions (figure 4.)

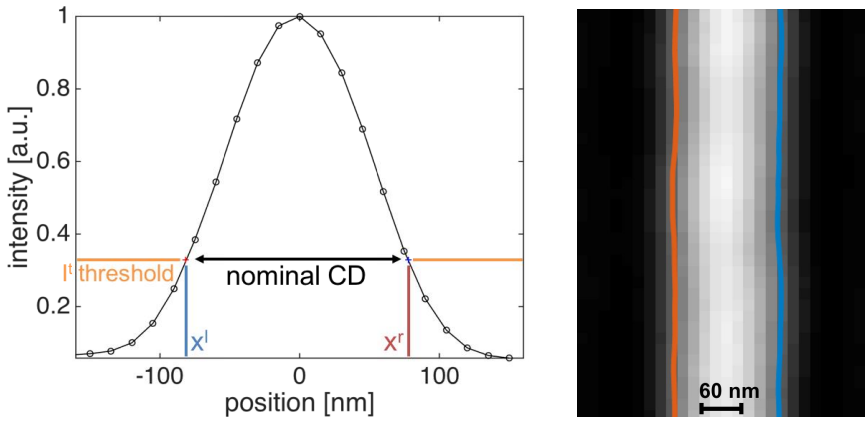

Figure 4. Determination of the line edges through threshold and interpolation. (left) One cross-section of an image acquired with 40 sec exposure time, a peak photon density of 40 photons/nm^2, and a partial coherence of 0.3; the effective pixel size is (dx*dy) = 15x15 nm^2. Circled dots are data points, and crosses are interpolated edge positions at the threshold. (right) Overlay of the aerial image and the retrieved left and right line edges for many different positions along the line.

Assuming that the line is vertical (y-direction), that $I(x,y) = I[n, m]$ is the intensity of the pixel at (integer) coordinate $\{n, m\}$ (with $(x, y) = (n*dx, m*dy)$), I_t is the threshold and n_{t+} the pixel index at the left-side of the threshold on the rising edge (figure 4), the left edge position for row m is approximately:

$$x^l[m] = \left(n_{t+} - \frac{I[n_{t+}, m] - I_t}{(I[n_{t+}, m] - I[n_{t+} - 1, m])}\right) * dx \qquad [1]$$

and similarly for the right edge (substituting n_{t+} for the falling edge.) This method of continuous edge-position interpolation (on pixel position) avoids the problem of discretization onto a finite grid before the threshold is applied, which is another approach to the row-by-row width calculation.

Left and right edges are determined individually, and the local width is calculated from their difference. The threshold for 160-nm line width corresponds to approximately one quarter of the peak intensity for $\sigma = 0.3$ and half of the peak intensity for $\sigma = 0.8$; the normalized image log-slope (NILS) values are 5.0 for $\sigma = 0.3$, 6.6 for $\sigma = 0.6$ and 3.0 for $\sigma = 0.8$.

Finally, we extracted (1) the same line from ten independent images recorded in sequence to assess the effects of shot noise, and analyzed (2) fourteen adjacent lines from the same image, to build the line statistics (figure 5.)

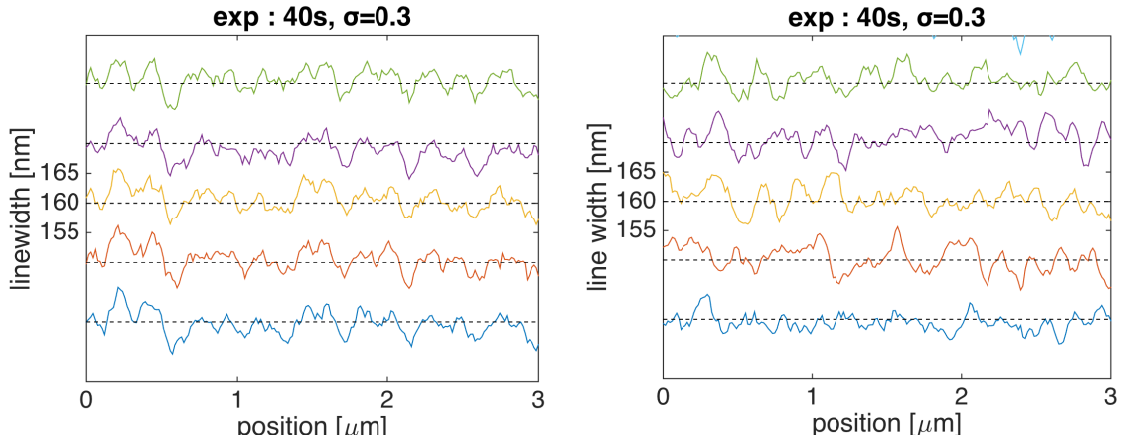

Figure 5. Line-width retrieval from aerial images using threshold and interpolation. Same line extracted from various repeated measurement (left) and various lines extracted from the same image (right). The lines have the same average nominal width but are offset for clarity.

4. INFLUENCE OF THE PHOTON NOISE ON MEASURED LINE-WIDTH ROUGHNESS

The noise in the acquired images impacts the line-edge retrieval [10] thus the overall measured line-width roughness *LWR,* by adding a contribution LWR_{photon} to the intrinsic roughness LWR_{mask} caused by the mask structure itself. Assuming they're statistically independent, the measured *LWR* can be expressed as :

$$LWR = \sqrt{LWR_{photon}^2 + LWR_{mask}^2} \qquad [2]$$

Line-width roughness is defined as three times ("3σ") the measured line-width standard deviation. Shorter exposure times, measurements yield noisy data (figure 6, left), but averaging multiple exposures allows us to capture the fine features of the intrinsic roughness, comparable to measurements made with longer exposure times (figure 6, right.)

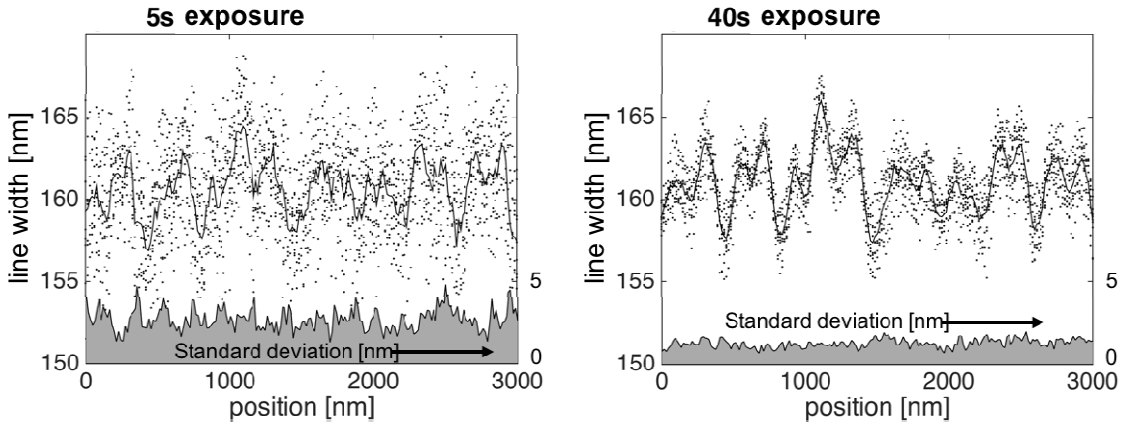

Figure 6. Influence of photon shot noise on the line-width and LWR measurement. Superposition of ten sequential measurements of the same dense line pattern with (left) 5 sec and (right) 40 sec exposure times, and σ = 0.3. Dots indicate the measured widths along the lines, while the solid line shows the row-average. The standard deviation at each position is indicated by the filled area below. The underlying (reproducible) line-width contour becomes apparent for longer exposure time (solid line).

The noise contribution to the measured LWR should scale as the of the inverse square root of the number of photons per pixel [10]. The measured LWR decreases as expected with exposure time (in this experiment, the detector sees approximately 64 photons/pixel/s at threshold for σ = 0.3) toward an asymptote (figure 7). At the highest exposure time,

the shot noise contribution becomes small compared to the intrinsic line-width roughness. We can estimate the intrinsic aerial image LWR by fitting the data and extracting the asymptote. For example, with σ = 0.3, we estimate the intrinsic LWR to be 5.8 nm for these lines.

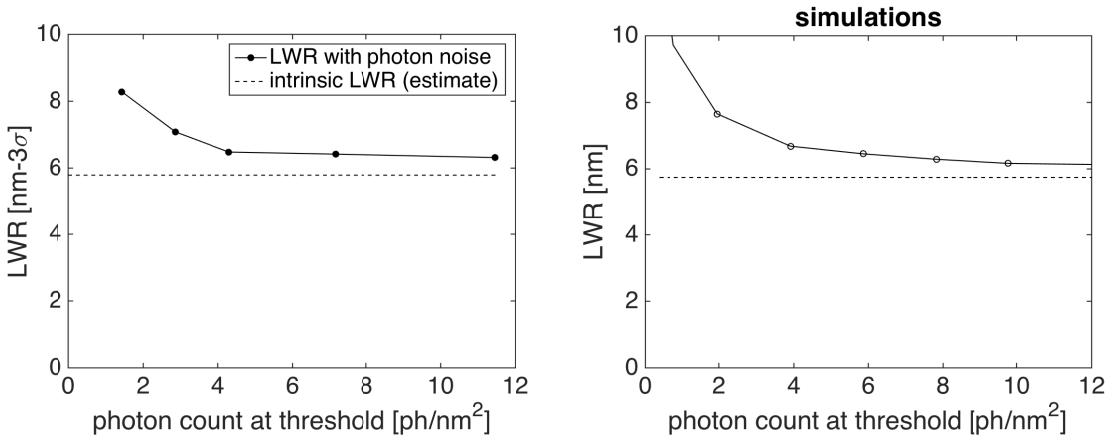

Figure 7. Influence of photon shot noise on the magnitude of the LWR, from measurement (left) and as predicted by simulations using corresponding physical parameters (right). Here, σ = 0.3, and the nominal line width is 160 nm. As the exposure time is increased, the inherent line-width roughness caused by the pattern and the mask blank roughness becomes dominant.

In the conditions of the experiment, the intrinsic LWR and the photon noise have a comparable impact on the aerial image LWR when the exposure is 15 seconds (photon density in the order of 4 photons/nm^2 at the nominal threshold; note that 1 photon/nm^2 at λ = 13.5 nm corresponds to 1.47 mJ/cm^2 on the mask side.) Since the noise in the image acquisition is limited by the physical process of photon counting (all external source of noise being negligible), the photon noise will affect printing in a stochastic fashion, increasing the aerial image LWR at low exposure dose.

5. EFFECT OF ILLUMINATION AND NILS

Generally speaking, coherence increases the NILS, and intensifies the presence of speckle. This is a manifestation of the spatial coherence caused by small phase variations from the reflective multilayer coating or underlying substrate. That is, incoherent illumination tends to blur the speckle, resulting in apparently smoother lines, in many cases. However, this decrease in sharpness comes with a higher sensitivity to photon noise for comparable level of incoming photon flux, eventually trading intrinsic edge roughness for stochastic roughness (figure 8.) that only affects aerial image measurement or printing in resist.

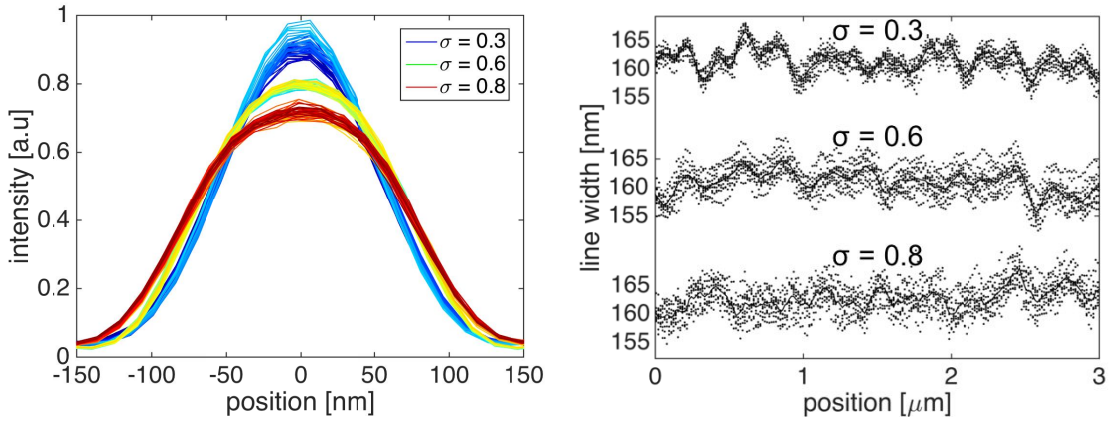

Figure 8. Effect of partial coherence on line-width roughness. (left) overlaid cross-sections for a line from a single measurement acquired with a .33 4xNA lens, 40 s exposure time and partial coherence σ = 0.3, σ = 0.6 and σ = 0.8; (right) overlaid line-width measurements for many measurements of the same line, for partial coherence σ = 0.3, σ = 0.6 and σ = 0.8. Lower coherence decreased speckle but increased sensitivity to photon noise.

There is however a slight advantage to incoherent illumination in that the roughness no longer has definite coherence length. In that respect, engineered partial coherence can be used [11] to reduce the sensitivity to some kind of defects such as bridging, that would be caused by mask roughness (attributable to a bright speck, akin to a slight phase defect.)

Another way to influence the line width is to change the intensity threshold. Since the interpolation is somewhat aggressive, with measured line-width variations smaller than the pixel size, changing the threshold by a small amount does not necessarily involve different image pixels, resulting in a linear scaling. However, the image is oversampled by a factor of 2.7 relative to the Nyquist limit, and the effective pixel size in our experiment is small enough to allow using pair-wise distinct interpolation points (figure 9, left.) Our experiment shows that there is no appreciable change in the LWR or sensitivity to photon noise while changing the threshold within ten percent: CD and CDU do not affect LWR or LCDU measurement (figure 9, right.)

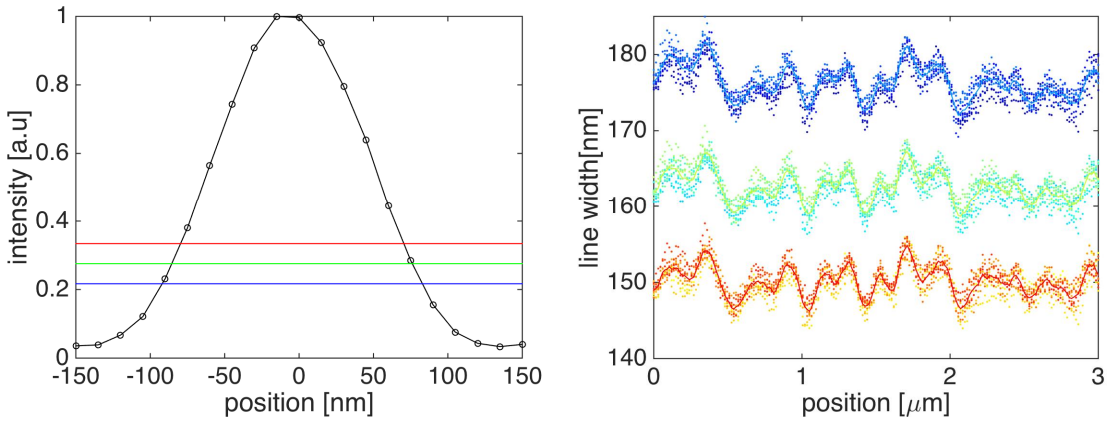

Figure 9. Aerial image line-width for various thresholds, with σ = 0.3 and 40 s exposure time. (left) cross-section of the line and thresholds; (right) corresponding lines-width along the line. The local roughness is not affected by more than the photon noise.

6. POWER SPECTRAL DENSITY

Comparing the line-width roughness of various lines in the same field allows us to estimate the power spectral density of the lines and their dependence on the imaging conditions (figure 10.)

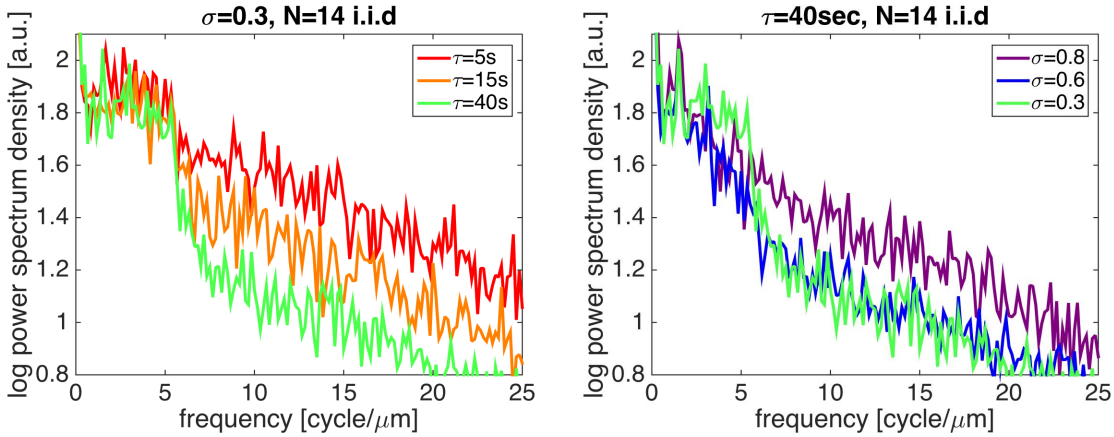

Figure 10. Power spectral density of the LWR (averaged over 14 contiguous lines), for various exposure times at σ = 0.3 (left) and for three different σ values at a long exposure time (right.) All lines are statistically independent and identically distributed (*i.i.d.*)

For longer exposure times and higher partial coherence settings ($\sigma = 0.3$), where the photon-noise contribution is small compared with the intrinsic LWR, it is possible to discern a sharp roll-off in the PSD at approximately 6 cycles/μm. We expect the limited numerical aperture (NA) of the lens to cause a spatial frequency cutoff near $\sin(4xNA/4)/\lambda = 6.11$ cycles/μm. Partial coherence (high σ) has the effect of the decreasing the steepness of the roll-off at higher spatial frequencies since there is less optical filtering, while the line width becomes more sensitive to photon-noise (which is not band-limited) at higher frequency.

7. CONCLUSION

Though resist line-edge roughness is generally governed by chemical processes (chemical shot noise, acidic diffusion), the roughness embedded in the aerial image, either as a replication of the mask pattern roughness, replicated surface roughness or photon noise, will continue to play a more significant role as pattern dimensions shrink. We have shown that it is possible to study the intrinsic aerial image LWR from actinic photo-mask imaging with sub-nanometer precision. In the examples presented, the conjunction of the illumination coherence and the intrinsic roughness of the mask creates speckle that cause LWR on the order of 5.8 nm on the mask side when studying a nominal CD of 160 nm, which can be measured using photon densities in excess of 4 photons/nm^2, at the threshold intensity level. In addition, we found that although incoherent illumination (i.e. higher σ values) reduces speckle amplitude, a smaller NILS makes measurements more sensitive to photon shot noise. The (repeatable) effect of the reproduced mask roughness is replaced by the (statistical) influence of the photon noise, and results seems to indicate that increased exposure time does not affect the minimum LWR set by speckle formation, reducing the impact of speckle mitigation [11]. We recognize that pattern size, threshold level, illumination and NA play a role in the final measured LWR, and require further investigation.

ACKNOWLEDGEMENT

We would like to thank Intel Corporation for the manufacturing of the mask used in these experiments, Suchit Bhattarai and Valeriy Yashchuk for fruitful discussions, and David Johnson for his participation in the data collection. The LBNL EUV program is supported by Eureka, and initial funding for SHARP was from SEMATECH. The Advanced Light Source is supported by the Director, Office of Science, Office of Basic Energy Sciences, of the U.S. Department of Energy under Contract No. DE-AC02-05CH11231.

REFERENCES

[1] George, S. A., Naulleau, P. P., Mochi, I., Salmassi, F., Gullikson, E. M., Goldberg K. A., Anderson, E. H., "Extreme ultraviolet mask substrate surface roughness effects on lithographic patterning," J. Vac. Sci. Technol., B 28(6), 23-30 (2010).
[2] Naulleau, P. P., "Relevance of mask-roughness-induced printed line-edge roughness in recent and future extreme-ultraviolet lithography tests," Appl. Opt. 43(20), 4025-4032 (2004).
[3] Naulleau, P. P. and Gallatin, G., "Spatial scaling metrics of mask-induced line-edge roughness," J. Vac. Sci. Technol., B 26(6), 1903-1910 (2008).
[4] Naulleau, P. P., George, S. A., "Implications of image plane line-edge roughness requirements on extreme ultraviolet mask specifications," Proc. SPIE 7379, 73790O1-11 (2009).
[5] Zweber, A. E., Gallagher, E., Sanchez, M., Senna, T., Negishi, Y., Konishi, T., McGuire, A., Bozano, L., Brock. P., Truong, H., "EUV Mask Line Edge Roughness," Proc. SPIE 8322, 83220O1-10 (2012).
[6] Pret, A. V., Gronheid, R., Engelen, J., Yan, P.-Y., Leeson M. J., Younkin, T. R. "Evidence of speckle in extreme-UV lithography," Appl. Opt. 20(23) 25970-25978 (2012).
[7] Yang, P.-Y., Zhang G., Gullikson, E. M., Goldberg, K. A., Benk, M. P., "Understanding EUV mask blank surface roughness induced LWR and associated roughness requirement," Proc. SPIE 9422, 94220J1-12 (2015).

[8] Goldberg, K. A., Mochi, I., Benk, M. P., Lin, C., Allezy, A., Dickinson, M., Cork, C. W., Macdougall, J. B., Anderson, E,. H., Chao, W., Salmassi, F., Gullikson, E., M., Zehm, D., Vytla, V., Cork, W., DePonte, J., Picchi, G., Pekedis, A., Katayanagi, T., Jones, M. G., Martin, E., Naulleau P. P., Rekawa, S. B., "The SEMATECH high-NA actinic reticle review project (SHARP) EUV mask-imaging microscope, " Proc. SPIE 8880, 88800T1-9 (2013).
[9] Mangat, P., Verduijn, E., Wood, O. R., Benk M. P., Wojdyla, A., Goldberg, K. A., "Mask blank defect printability comparison using optical and SEM mask and wafer inspection and bright field actinic mask imaging," Proc. SPIE 9658, 96580E1-8 (2015).
[10] Wintz, D. T., Goldberg, K. A., Mochi, I., Huh, S., "Photon flux requirements for extreme ultraviolet reticle imaging in the 22- and 16-nm nodes," J. Micro/Nanolith. MEMS MOEMS 9(4), 041205-1-8 (2010)
[11] McClinton, B. M. and Naulleau, P. P., "Mask roughness induced LER control and mitigation: aberrations sensitivity study and alternate illumination scheme," Proc. SPIE 7969, 79691Z1-11 (2011)